

# Dielectric Studies of Water Clusters in Cyclodextrins: Relevance to the Transition between Slow and Fast Forms of Thrombin

Stephen Bone<sup>†</sup>

*Institute for Bioelectronic and Molecular Microsystems, University of Wales Bangor, Dean Street, Bangor LL57 1UT, Gwynedd, United Kingdom*

*Received: June 19, 2006; In Final Form: August 7, 2006*

Cyclodextrins are useful models in the study of hydrogen bonded water clusters. In  $\alpha$ -cyclodextrin hexahydrate ( $\alpha$ -CD $\cdot$ 6H<sub>2</sub>O), water molecules are ordered and occupy well-defined positions whereas in the larger  $\beta$ -cyclodextrin dodecahydrate ( $\beta$ -CD $\cdot$ 12H<sub>2</sub>O), there is considerable disorder with water molecules freely arranged over several possible sites. Here it is shown that  $\beta$ -CD exhibits substantial structural flexibility and proton mobility compared with  $\alpha$ -CD which is relatively very rigid and exhibits negligible short-range protonic conduction. These properties are directly controlled by the effective dielectric constant of the molecule, which is determined by the rotational freedom of water molecules in the hydrogen bond network. This model may be relevant to proteins where water clusters of this kind are found on the protein surface and occasionally in the protein interior. The case of thrombin, an allosteric enzyme incorporating a network of 20 internal hydrogen bonded water molecules, is discussed.

## Introduction

$\beta$ -Cyclodextrin is a cyclic sugar composed of seven linked glucoses that crystallizes from water with 11 or 12 associated water molecules. These waters, both enclosed within the cavity and interstitial, are highly disordered being distributed over 16 possible hydration sites.<sup>1–3</sup> Two primary hydroxyl groups are also disordered. In this case, water positions and hydrogen bonding are freely arranged rather than being constrained by symmetry requirements.

$\alpha$ -Cyclodextrin is a smaller molecule with 6 glucoses binding 6 water molecules in a lattice-independent hydrogen bond configuration.<sup>4,5</sup> All waters and hydroxyl groups are ordered and well-defined positions are fully occupied with water molecules engaged in at least 3 hydrogen bonding contacts.

Previous dielectric studies on cyclodextrin hydrates have been confined to thermally stimulated depolarization methods and to low-frequency measurements which are sensitive to ionic and interfacial polarization processes and which generally produce large dielectric responses.<sup>6,7</sup> In this work, high-frequency dielectric measurements, over the frequency range 1 MHz to  $\sim$ 20 GHz, were performed. These are sensitive to dipolar relaxation processes and short-range proton migration.<sup>8</sup>  $\alpha$ - and  $\beta$ -cyclodextrins were studied as model systems<sup>1,4</sup> to gain an insight into the types of hydrogen bonded water clusters which might be supported in proteins and the effect of these on the dynamics of protein molecules. This scheme may be relevant to proteins where water clusters of this kind are found on the protein surface<sup>9–12</sup> and occasionally in the protein interior.<sup>13,14</sup> In particular, the allosteric enzyme thrombin incorporates a channel containing a network of 20 hydrogen bonded water molecules which appear to play an important role in the mechanism of enzyme action.

The activity of thrombin, an allosteric serine protease, is determined by binding of Na<sup>+</sup> to a specific binding site.<sup>15–17</sup>

The Na<sup>+</sup>-bound fast form of thrombin plays a procoagulant role in blood cleaving fibrinogen with a high specificity while the Na<sup>+</sup>-free slow form<sup>18,19</sup> has an anticoagulant function with specificity toward protein C.<sup>15,18</sup> Na<sup>+</sup> binding to the slow form triggers a number of changes in the orientation of side chains in the channel region to produce the fast form.<sup>15–19</sup> The Na<sup>+</sup> binding site, active site, and substrate binding pocket are all spatially separate and located at various positions in the channel containing the water network.<sup>20–23</sup> The water molecules and many of the side chains which define the channel are highly conserved indicating their importance to the activity of the enzyme.<sup>20,21</sup> Mutations of channel side chains have been shown to produce effects which are evident at sites in the channel up to 1.7 nm away indicating a thermodynamic linking of these groups.<sup>20,22</sup> The exact mechanism responsible for translating Na<sup>+</sup>-binding into the allosteric changes which result in the transition from slow to fast form of the enzyme is not understood but has been clearly linked to a significant rearrangement of the network of water molecules.<sup>21,22</sup> In this work, the nature of the hydrogen bonded network of water molecules in the channel and the possible implications for structural mobility in thrombin are discussed with reference to the experimental data collected for hydrogen bonded water clusters in  $\alpha$ - and  $\beta$ -cyclodextrin. A scheme is proposed whereby Na<sup>+</sup> binding is coupled to allosteric shifts in the enzyme.

## Experimental Methods

**Theoretical.** For dipolar orientational relaxation in materials at low levels of hydration, the Onsager correction for local electric field is relevant. The corrected magnitude of the dielectric dispersion,  $F(\epsilon)$ , as developed by Kirkwood, Fröhlich, and others is given by<sup>24</sup>

$$F(\epsilon) = \frac{(\epsilon_s - \epsilon_\infty)(2\epsilon_s + \epsilon_\infty)}{\epsilon_s(\epsilon_\infty + 2)^2} = \frac{Ng\langle\bar{u}\rangle^2}{9\epsilon_0 kT} \quad (1)$$

<sup>†</sup> Address correspondence to the author at the following: fax +44 (0)-1248 361429, e-mail s.bone@informatics.bangor.ac.uk.

where  $\epsilon_s$  and  $\epsilon_\infty$  are the limiting low- and high-frequency permittivity values of each dispersion and  $\epsilon_0$  is the permittivity of free space.  $N$  is the number density of dipoles,  $\langle \bar{\mu} \rangle$  is the mean effective dipole moment, and the Kirkwood correlation factor,  $g$ , accounts for correlated dipole motion ( $g \geq 1$  and has a value of unity for uncorrelated dipoles).

The characteristic relaxation time,  $\tau$ , as derived by Eyring, is given by

$$\tau = \frac{1}{2\pi f} = \frac{h}{kT} \exp\left(\frac{\Delta G}{RT}\right) = \frac{h}{kT} \exp\left(-\frac{\Delta S}{R}\right) \exp\left(\frac{\Delta H}{RT}\right) \quad (2)$$

where  $f$  is the relaxation frequency and  $\Delta G$ ,  $\Delta H$ , and  $\Delta S$  are the activation free energy, enthalpy, and entropy of the relaxation process.

The dielectric permittivity and loss characteristics were modeled by using a superposition of dispersions,<sup>25</sup> each represented by  $J_k(\omega)$  where the complex permittivity  $\epsilon^*$  is given by

$$\epsilon^*(\omega) = \epsilon'(\omega) - i\epsilon''(\omega) = \epsilon_\infty + \sum_{k=1}^k J_k(\omega) \quad (3)$$

If the relaxation time and magnitude of each dispersion is denoted by  $\tau_k$  and  $M_k$  then

$$J_k(\omega) = \frac{M_k}{1 + (i\omega\tau_k)^{1-\alpha}} \quad (4)$$

where  $\alpha$  is included to account for a distribution of relaxation times ( $0 \leq \alpha \leq 1$ ).

**Materials.**  $\alpha$ - and  $\beta$ -cyclodextrin were obtained from Sigma-Aldrich Co. (Poole, Dorset) and were recrystallized from ultrapure water or deuterium oxide (Sigma-Aldrich). Methyl- $\beta$ -cyclodextrin and 2-hydroxypropyl- $\beta$ -cyclodextrin were purchased from Sigma-Aldrich and were used without further treatment.

Dielectric measurements over the frequency range 1 MHz to approximately 20 GHz were performed by using a technique known as time-domain reflectometry (TDR). In a typical TDR experiment a train of voltage steps of magnitude 500 mV and rise time 25 ps is transmitted from a tunnel diode down a low-loss coaxial line terminated by a piece of air-line containing the sample. In the particular method used (the precision difference method<sup>26</sup>), the reflected voltage waveform from the sample is compared with that from a reference dielectric of known complex permittivity. By using the appropriate time windows and sample cell lengths and after suitable transformation from time to frequency domain, it is possible to accurately determine the dielectric characteristics of the sample. For the frequency range 1 MHz to 1 GHz, data were analyzed over a 140 ns time window, using a coaxial sample cell length of 5 mm with inner and outer electrode diameters of 5 and 7 mm, respectively. For frequencies between 0.5 and 20 GHz, a time window of 5 ns and effective cell length of 0.2 mm were employed. A digital storage oscilloscope (Hewlett-Packard 54120A) with 4 channel test set (HP 54121A), which includes a dedicated TDR test port, was employed for data capture.

For hydration measurements, cyclodextrin samples of density  $\sim 9.5 \times 10^5 \text{ g m}^{-3}$  were exposed to step increases in hydration over the range 0% to 85% relative humidity, where 0% was considered to be the state reached after the sample had been in equilibrium with a vacuum of  $1 \times 10^{-2}$  mbar for 24 h. Water partial pressures were measured with a Honeywell humidity sensor (type HIH-3610), which had been previously calibrated

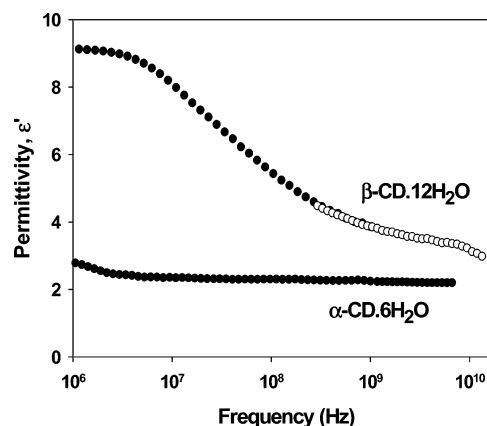


**Figure 1.** High-frequency dielectric characteristics of  $\alpha$ -cyclodextrin-6H<sub>2</sub>O and  $\beta$ -cyclodextrin-12H<sub>2</sub>O crystals; variation of the real component of the complex permittivity,  $\epsilon'$ , with frequency at 295 K. Closed symbols represent data collected in a 140 ns time window for a coaxial sample cell length of 5 mm (inner and outer electrode diameters 5 and 7 mm, respectively), and open symbols indicate a 5 ns time window and effective cell length of 0.2 mm.

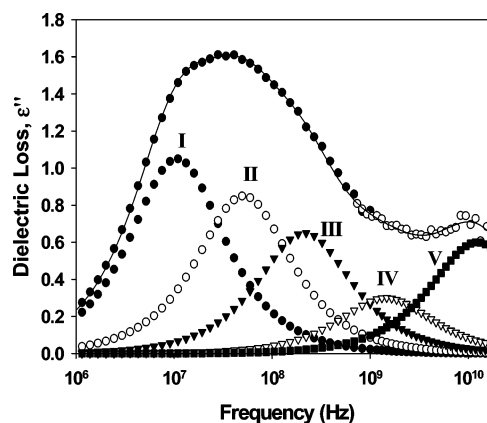


**Figure 2.** High-frequency dielectric characteristic of  $\beta$ -cyclodextrin-12H<sub>2</sub>O crystals; variation of the imaginary component of the complex permittivity (dielectric loss),  $\epsilon''$ , with frequency at 295 K. The solid line is the sum of the individual components. Experimental details are identical with those for Figure 1.

with saturated salt solutions. Hydration isotherms of  $\beta$ -CD were produced with a Sartorius vacuum microbalance (type 4133).

## Results

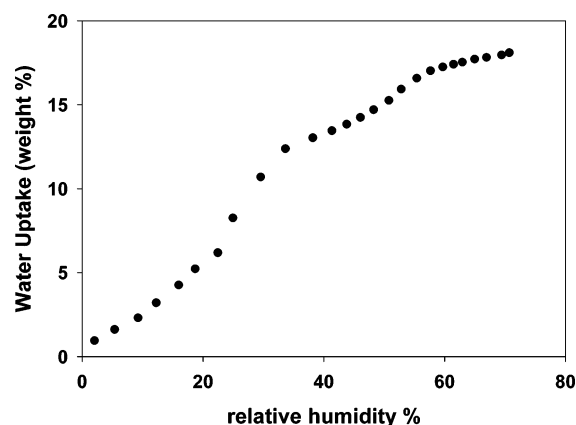
The difference between the high-frequency permittivity (otherwise known as the dielectric constant) characteristics of crystalline  $\alpha$ - and  $\beta$ -cyclodextrin is marked as shown in Figure 1.  $\alpha$ -CD shows permittivity values which are low and virtually unchanging over the whole frequency range and in this case there is a complete absence of any relaxation behavior.<sup>38</sup> The relatively high permittivity values exhibited by  $\beta$ -CD extend from 1 MHz to 20 GHz and indicate the presence of a number of relaxation processes. These can be identified more easily from Figure 2, which shows the corresponding experimentally determined dielectric loss and constituent dispersions obtained from modeling with use of eqs 3 and 4. The data for  $\alpha$ -CD have been omitted for clarity but values of  $\epsilon'' < 0.03$  were recorded over the entire measurement frequency range. Table 1 gives details of the dielectric parameters of each of the component dispersions used to fit the experimental data.

In the case of  $\beta$ -CD, four relaxation processes were unambiguously identified. It was found that dispersions I, II, III, and

**TABLE 1: Dielectric Parameters of Component Dispersions for  $\beta$ -Cyclodextrin $\cdot$ 12H<sub>2</sub>O at 295 K<sup>a</sup>**

	dispersion I	dispersion II	dispersion III	dispersion IV	dispersion V
$\epsilon_s$	$9.15 \pm 0.15$	$7.05 \pm 0.12$	$5.35 \pm 0.07$	$4.05 \pm 0.06$	$3.45 \pm 0.05$
$\epsilon_i$	$7.05 \pm 0.12$	$5.35 \pm 0.07$	$4.05 \pm 0.06$	$3.45 \pm 0.05$	$2.25 \pm 0.06$
$M$	$2.1 \pm 0.19$	$1.7 \pm 0.14$	$1.3 \pm 0.09$	$0.6 \pm 0.08$	$1.2 \pm 0.08$
$\tau$ (ns)	$14.8 \pm 0.4$	$3.1 \pm 0.1$	$0.74 \pm 0.02$	$0.11 \pm 0.1$	$0.013 \pm 0.001$

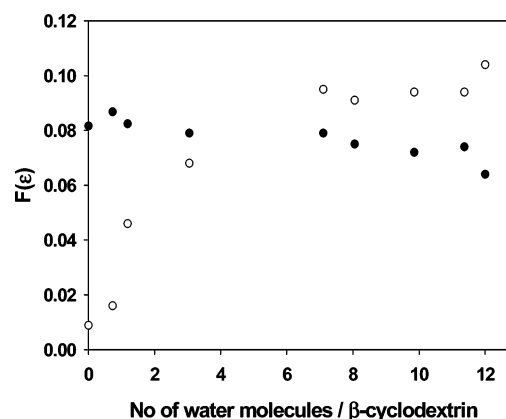
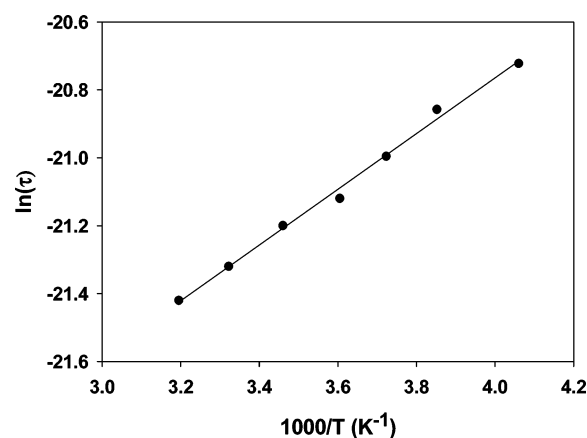
<sup>a</sup>  $\epsilon_s$  and  $\epsilon_i$  are the low- and high-frequency permittivities,  $M$  is the magnitude (eq 4), and  $\tau$  is the characteristic relaxation time of each of the component dispersions. Errors are given as  $\pm 1$  s.

**Figure 3.** Hydration isotherm for  $\beta$ -cyclodextrin at 295 K.

V were required for successful modeling of the experimental data without resorting to unrealistic values of  $\alpha$  ( $>0.5$ ). For data fitting to four relaxation processes, values of  $\alpha$  for dispersions III and V varied in an unpredictable manner with temperature and hydration. Optimal modeling of the experimental data could only be achieved by including dispersion IV. In this case data were successfully modeled for all temperatures and hydration values by using single Debye relaxations ( $\alpha = 0$ ). In all cases modeling was simultaneously performed on data in three representations:  $\epsilon'$  vs log frequency,  $\epsilon''$  vs log frequency, and  $\epsilon'$  vs  $\epsilon''$  (Cole–Cole plot).

Crystallizing  $\beta$ -CD from D<sub>2</sub>O produced increases in the relaxation times of dispersions I and II by factors of  $1.38 \pm 0.05$  and  $1.41 \pm 0.04$ , respectively. A shift in frequency by  $\sqrt{2}$  is expected to originate from a process involving nuclear masses which have undergone H/D exchange. Dispersions I and II must therefore be associated with proton translocation as opposed to the relaxation of water molecules or hydroxyl groups. Both dispersions exhibit temperature-independent relaxation times (temperature range 246 to 313 K) indicating that the free energy changes associated with these relaxation processes are zero. The dielectric properties of  $\beta$ -CD were also studied as a function of water content and in this case the hydration isotherm (Figure 3) was used to ascertain the hydration level. For all  $\beta$ -CD crystal samples used, 12 water molecules were found to be associated with each cyclodextrin. The variation of dispersion magnitudes with hydration level is described by Figure 4. For dispersion I, the proton pathways appear to be primarily associated with the  $\beta$ -CD sugar moieties since the dispersion magnitude is independent of the hydration level. However, dispersion II increases linearly but saturates above approximately 5 water molecules per cyclodextrin indicating that this proton relaxation process involves a number of key water molecules.

By contrast with dispersions I and II, the relaxation time of dispersion III is temperature dependent as shown in Figure 5 indicating, for  $\beta$ -CD $\cdot$ 12H<sub>2</sub>O, an activated relaxation process with a relatively low activation enthalpy of 1.6 kcal mol<sup>-1</sup>. The dispersion magnitude also increases linearly with increasing

**Figure 4.** Dependence of dielectric parameter  $F(\epsilon)$  (eq 1) of dispersions I (closed symbols) and II (open symbols) on hydration level of  $\beta$ -cyclodextrin at 295 K.**Figure 5.** Activation plot for dispersion III of  $\beta$ -cyclodextrin $\cdot$ 12H<sub>2</sub>O.

temperature. This is consistent with dipolar relaxation where thermal energy gives rise to an increase in the effective dipole moment as a result of greater structural mobility. Figure 6 shows the dependence of the dielectric parameter and relaxation frequency as a function of the number of water molecules associated with  $\beta$ -CD.  $F(\epsilon)$  initially increases linearly with increasing water content while the relaxation frequency falls with increasing hydration. For fully hydrated  $\beta$ -CD, the free energy change  $\Delta G = 4.7$  kcal mol<sup>-1</sup>, which is made up of a change in enthalpy  $\Delta H = 1.6$  kcal mol<sup>-1</sup> and an entropy term  $T\Delta S = -3.1$  kcal mol<sup>-1</sup>. Dispersion III is considered likely to be related to mobility in the cyclodextrin structure. It may be attributed to orientational relaxation of hydrogen bonded hydroxyl groups located around the inside of the  $\beta$ -CD cavity and a methylol group protruding from the outer ring structure. The hydration dependence of the dispersion magnitude is due to a reduction of the potential barrier associated with the relaxation process. Methylation of the majority of hydroxyl and methylol groups, resulting in a decrease in the dipole moment of each group, causes a dramatic reduction in the relative magnitude of dispersion III. Replacement by hydroxypropyl CH<sub>2</sub>CHOHCH<sub>3</sub>

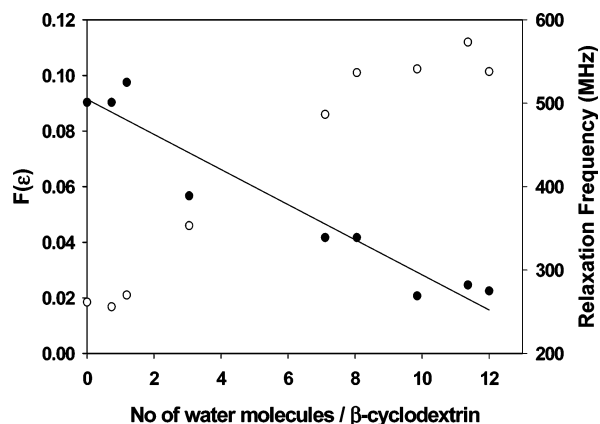


**Figure 6.** Variation of the dielectric parameter  $F(\epsilon)$  (open symbols) and relaxation frequency (closed symbols) of dispersion III for  $\beta$ -cyclodextrin with hydration level at 295 K.

groups affects the relaxation time of dispersion III only, producing an increase from 0.74 to 1.13 ns. Alternatively, the dispersion may originate from the cyclodextrin ring structure with permanent dipoles resulting from charge separation due to the glucose ring oxygens and reorientational motion possible via flexible glycosidic bonds.

In addition to these dispersions, two other processes are described by the data. These dispersions (IV and V) centered at 1.45 and 12.3 GHz are similar to those appearing in the high frequency dielectric characteristics of chemically dissimilar systems such as hydrated polyaspartic acid and polyasparagine (Bone, S., unpublished data) and silica gels<sup>27</sup> and it seems likely that they originate from the relaxation of hydrogen bonded water. The relaxation time of dispersion V also compares favorably with those found for protein bound water in neutron scattering<sup>28</sup> and in femtosecond-resolved fluorescence studies on DNA.<sup>29</sup>

Detailed neutron diffraction studies<sup>2</sup> have described the complex nature of the disordered water structure in  $\beta$ -CD $\cdot$ 11H<sub>2</sub>O. Based on the occupancies of the hydration sites and two disordered primary hydroxyl groups, the proportion of single and multiple hydrogen bonded water at any instant can be estimated. Approximately 6 water molecules/ $\beta$ -CD are doubly H-bonded with 4 water molecules/ $\beta$ -CD connected via three or four hydrogen bonds and only 1 water is on average singly hydrogen bonded to  $\beta$ -CD. Despite the existence of these different populations of hydrogen bonded water, the dielectric data produces a linear hydration characteristic, as described in Figure 7, indicating that polarization of the water molecules occurs to a similar extent over the whole hydration range. This may be due to rapid exchange of water molecules between hydration sites with residence times which are short compared to the measurement time giving rise to characteristics reflecting a time averaging of the hydration scheme.

Unfortunately, for technical reasons and because of the relatively small size of dispersion IV and nearness to the experimental high-frequency limit of dispersion V, it was not possible to accurately determine the activation enthalpies of these processes. However, the values estimated for these dispersions are relatively small ( $<1$  kcal mol<sup>-1</sup>) and considerably smaller than that associated with the breaking of a hydrogen bond ( $\sim 4.5$  kcal mol<sup>-1</sup>), which is thought to occur with rotational reorientation of water molecules in bulk water. For the water associated with  $\beta$ -CD, it is possible that the relatively small electric field induced reorientations do not break or significantly weaken hydrogen bond interactions. It has been

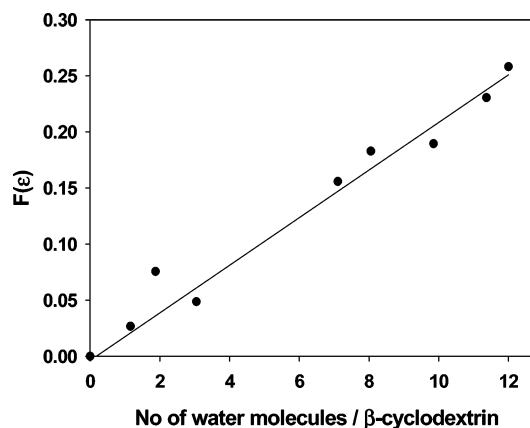


**Figure 7.** Dielectric parameter  $F(\epsilon)$  (eq 1) for dispersion V of  $\beta$ -cyclodextrin as a function of hydration at 295 K.

shown<sup>30</sup> that small deviations in the bond angle of up to 20° have a relatively minor effect on hydrogen bond strength. Alternatively, hydrogen bonds broken during reorientation may rapidly reform in an energetically similar configuration resulting in a relatively small net change in enthalpy. This would be favored energetically and would be consistent with the relatively freely arranged hydrogen bonding scheme in  $\beta$ -CD in which water molecules are able to flip between similar hydrogen bonding configurations.<sup>1</sup>

It has not been possible to assign dispersion IV to a particular relaxation process. However, it may be derived from one of the cross correlation terms generated through interaction between two of the processes responsible for other dispersions. It is now known from experimental<sup>31</sup> and simulation<sup>32,33</sup> studies that coupled phenomena of this type can produce dielectric dispersions although the relaxation frequencies and magnitudes are often difficult to predict.

## Discussion

Given the relatively open structure of  $\beta$ -CD compared with the more compact  $\alpha$ -CD, the greater molecular mobility of the former molecule is to be expected. However, it is evident from the hydration data that the proton translocation described by dispersion II and molecular flexibility reflected in dispersion III are considerably enhanced by inclusion of water in the case of  $\beta$ -CD but remain negligibly low for  $\alpha$ -CD. The hydrogen bonding hydration schemes of the two molecules are quite different and are responsible for the differences in behavior.  $\alpha$ -CD is able to form a well-defined hydrogen bonded water network with each ordered water molecule making 3 or 4 hydrogen bonds. Although exchange between hydration sites is still likely, residence times are expected to be relatively long compared with the measurement time scale. In  $\beta$ -CD, the water molecules are disordered and engaged in single and multiple hydrogen bonds in a variety of different configurations. Importantly, a proportion of these are rotationally mobile and therefore polarizable. This produces relatively high local permittivities and effective screening of inter- and intramolecular electrostatic interactions between polar species (e.g., hydroxyl and methylol groups) resulting in significant flexibility of the molecular structure. By contrast the 6 water molecules bound to  $\alpha$ -cyclodextrin cannot be detected in the frequency range covered and it must be concluded that these are irrotationally bound on the micro- to picosecond time scales covered.  $\alpha$ -CD therefore exhibits a low permittivity, the absence of mobile, high-permittivity water resulting in a relatively rigid molecular arrangement.



These systems indicate the critical influence of internal water clusters on the behavior of the molecule as a whole. The principles described here are also likely to be important in larger, more complex molecules such as proteins. Both molecular dynamics and proton translocation are known to be implicated in biological activity. A detailed review has recently been published in which the correlation between the activity of a number of globular and membrane proteins and protein internal motions is discussed.<sup>34</sup> In addition, computer simulation studies have linked the transition temperature for the onset of these motions in ribonuclease and myoglobin to the dynamics of protein-bound water.<sup>35,36</sup> This scheme may be particularly pertinent to proteins which incorporate clusters of water molecules into their internal structure. As described earlier, a prime example is the enzyme thrombin in which the binding of Na<sup>+</sup> to a site in a channel containing 20 internal water molecules triggers a transition between the slow (S) and fast (F) forms of the enzyme.

It has been proposed that the hydrogen bonded network of water molecules in the thrombin channel provides a thermodynamic link between the Na<sup>+</sup> binding site and the side chains involved in allosteric shifts<sup>21</sup> but a mechanism for translation of Na<sup>+</sup> binding to the structural changes has not yet been elucidated. It is known that Na<sup>+</sup> binding to the S form produces a dramatic reorganization of water in the channel. Four additional waters are bound in the F compared to the S form and in the F form all water molecules are ordered in a well-defined hydrogen bonded network<sup>21</sup> of the type exhibited by  $\alpha$ -cyclodextrin.

On Na<sup>+</sup> binding to the cation binding site of the S form of thrombin, a number of sequential changes with different time signatures can be expected to occur. In the scheme proposed, four water molecules are immediately engaged in providing the coordination hydration of the ion. This local structuring of water around the ion is considered likely to cause considerable disruption of the hydrogen bonding of the other water molecules in the channel. The resulting disorder is followed by a rearrangement of water molecules to form the ordered hydrogen bond network that is characteristic of the F-form of thrombin. Critical to the formation of the water network is the allosteric reorientation of side chains in the channel, which allows optimal hydrogen bonding with channel water molecules. Key groups in the channel which reorient to engage in hydrogen bonding are Asp<sup>189</sup> which shifts to form new hydrogen bonds with water in the middle of the channel and Ser<sup>195</sup> and Glu<sup>192</sup> which significantly reposition to hydrogen bond W<sup>915</sup>, a water molecule absent from the S-form, which extends the hydrogen bond network.<sup>21</sup>

A number of changes in enthalpy and entropy can be expected to accompany the S–F transition. Formation of the hydrogen bond network and effective charge compensation will result in a large decrease in enthalpy. There will also be an energetically unfavorable loss of entropy associated with ordering of the channel water. However, this will be compensated to some extent by a favorable change in  $\Delta S$ , indicated from X-ray crystallographic temperature coefficients,<sup>21</sup> which show that, in general, the side chains of the F-form of thrombin are significantly more disordered than in the S-form.

Although energetically unfavorable in isolation, the allosteric shifts in side chain orientation are expected to elicit, and be driven by, a net lowering of  $\Delta G$ , primarily through their facilitating the formation of the hydrogen bond network of water molecules. The scheme involving initial Na<sup>+</sup>-induced disruption of channel water followed by the formation of an enhanced

hydrogen bonded water network requiring reorientation of key side chains provides a possible explanation for the coupling of Na<sup>+</sup> binding to the allosteric changes. A similar reduction of free energy associated with stabilization of protein internal charge by means of local conformational changes has been recently reported for mutant forms of staphylococcal nuclease.<sup>37</sup>

X-ray crystallographic temperature factors indicate that channel water mobilities are low in both S- and F-forms,<sup>21</sup> suggesting a relatively low permittivity environment and consequently a more rigid molecular structure. This is consistent with data indicating that side groups in the channel occupy well-defined positions and are relatively immobile.<sup>21</sup> These conditions would seem to militate against there being sufficient structural flexibility in the protein interior to allow the allosteric shifts of the side chains to occur. However, these reorientations may be facilitated by the transient disorder of the channel water molecules immediately following Na<sup>+</sup> binding. As in the case of  $\beta$ -cyclodextrin, this would be expected to elicit flexibility in the local structure and therefore lower the energy required for these realignments. Release of Na<sup>+</sup> and its coordination water is similarly likely to disrupt the F-form hydrogen bond network causing a transient disordering of the water molecules and facilitating the reverse transition from F- to S-form.

**Acknowledgment.** I would like to thank Mr. R. B. Owen, Dr. L. Kuncheva, and Prof. R. Pethig for valuable discussions and Mr. I. Jones for technical assistance.

## References and Notes

- (1) Saenger, W.; Betzel, C.; Hingerty, B.; Brown, G. M. *Nature* **1982**, 296, 581.
- (2) Betzel, C.; Saenger, W.; Hingerty, B. E.; Brown, G. M. *J. Am. Chem. Soc.* **1984**, 106, 7545.
- (3) Klar, B.; Hingerty, B.; Saenger, W. *Acta Crystallogr.* **1980**, B36, 1154.
- (4) Saenger, W. *Nature* **1979**, 279, 343.
- (5) Lesyng, B.; Saenger, W. *Biochim. Biophys. Acta* **1981**, 678, 408.
- (6) Johari, G. P. *J. Mol. Struct.* **1991**, 250, 351.
- (7) Anagnostopoulou-Konsta, A.; Apekis, L.; Tsoukaris, G. *IEEE Trans. Electr. Insul.* **1992**, 27, 801.
- (8) Pethig, R. *Annu. Rev. Phys. Chem.* **1972**, 43, 177.
- (9) Bone, S.; Pethig, R. *J. Mol. Biol.* **1982**, 157, 571.
- (10) Bone, S.; Pethig, R. *J. Mol. Biol.* **1985**, 181, 323.
- (11) Bone, S. *Biochim. Biophys. Acta* **1987**, 916, 128.
- (12) Bone, S. *Phys. Med. Biol.* **1996**, 41, 1265.
- (13) Yu, B.; Blaber, M.; Gronenborn, A. M.; Clore, G. M.; Caspar, D. L. D. *Proc. Natl. Acad. Sci.* **1999**, 96, 103.
- (14) Sanschagrin, P. C.; Kuhn, L. A. *Protein Sci.* **1998**, 7, 2054.
- (15) Di Cera, E.; Guinto, E. R.; Vindigni, A.; Dang, Q. D.; Ayala, Y. M.; Wuyi, M.; Tulinsky, A. *J. Biol. Chem.* **1995**, 270, 22089.
- (16) Zhang, E.; Tulinsky, A. *Biophys. Chem.* **1997**, 63, 185.
- (17) Griffon, N.; Di Stasio, E. *Biophys. Chem.* **2001**, 90, 89.
- (18) Pineda, A. O.; Savvides, S. N.; Waksman, G.; Di Cera, E. *J. Biol. Chem.* **2002**, 277, 40177.
- (19) Carrell, C. J.; Bush, L. A.; Mathews, F. S.; Di Cera, E. *Biophys. Chem.* **2006**, 121, 177.
- (20) Krem, M. M.; Prasad, S.; Di Cera, E. *J. Biol. Chem.* **2002**, 277, 40260.
- (21) Pineda, A. O.; Carrell, C. J.; Bush, L. A.; Prasad, S.; Caccia, S.; Chen, Z.-W.; Mathews, S.; Di Cera, E. *J. Biol. Chem.* **2004**, 279, 31842.
- (22) Di Cera, E. *C. R. Biol.* **2004**, 327, 1065.
- (23) Di Cera, E. *J. Biol. Chem.* **2006**, 281, 1305.
- (24) Hill, N. E.; Vaughan, W. E.; Price, A. H.; Davies, M. *Dielectric Properties and Molecular Behaviour*; Van Nostrand Reinhold: London, UK, 1969.
- (25) Böttcher, C. J. F.; Bordewijk, P. *Theory of Dielectric Polarisation*; Elsevier: Amsterdam, The Netherlands, 1973.
- (26) Nakamura, H.; Mashimo, S.; Wada, A. *Jpn. J. Appl. Phys.* **1982**, 21, 467.
- (27) Sakamoto, T.; Nakamura, H.; Uedaira, H.; Wada, A. *J. Phys. Chem.* **1989**, 93, 357.

- (28) Perez, J.; Zanotti, J.-M.; Durand, D. *Biophys. J.* **1999**, 77, 454.
- (29) Pal, S. K.; Zhao, L.; Zewail, A. H. *Proc. Natl. Acad. Sci.* **2003**, 100, 8113.
- (30) Rao, C. N. R. In *Water; A Comprehensive Treatise*; Franks, F., Ed.; Plenum Press: New York, 1972; p 93.
- (31) Volmari, A.; Weingärtner, H. *J. Mol. Liq.* **2002**, 98–9, 293.
- (32) Ladanyi, B. M.; Skaf, M. S. *J. Phys. Chem.* **1996**, 100, 1368.
- (33) Weingärtner, H.; Knocks, A.; Boresch, S.; Hocht, P.; Steinhauser, O. *J. Chem. Phys.* **2001**, 115, 1463.
- (34) Daniel, R. M.; Dunn, R. V.; Finney, J. L.; Smith, J. C. *Annu. Rev. Biophys. Struct.* **2003**, 32, 69.
- (35) Tarek, M.; Tobias, D. J. *Biophys. J.* **2000**, 79, 3244.
- (36) Tournier, A. L.; Xu, J.; Smith, J. C. *Biophys. J.* **2003**, 85, 1871.
- (37) Denisov, V. P.; Schlessman, J. L.; Garcia-Moreno E., B.; Halle, B. *Biophys. J.* **2004**, 87, 3982.
- (38) The small rise in permittivity in the low-frequency part of Figure 1 indicates the presence of a relaxation process below 1 MHz.